

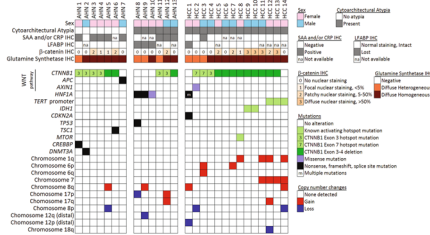
# INSIDE THE USCAP JOURNALS

<https://doi.org/10.1038/s41374-019-0328-4>

## MODERN PATHOLOGY

### Genomic analysis of atypical hepatocellular neoplasms

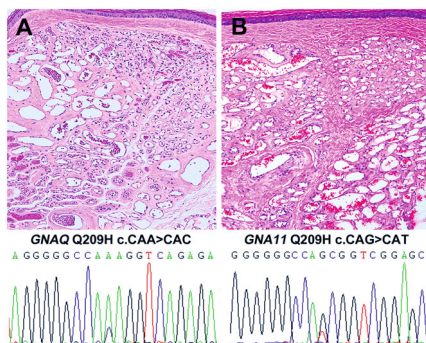
<https://doi.org/10.1038/s41379-019-0282-0>



There is a poorly recognized and characterized group of atypical hepatocellular neoplasms that fall between the WHO classifications of hepatocellular adenoma and carcinoma. Joseph et al. examined 27 hepatocellular neoplasms (14 carcinomas and 13 atypical neoplasms) showing diffuse glutamine synthetase staining (surrogate marker for activated  $\beta$ -catenin). Capture-based next-generation sequencing was performed across the samples to assess genomic alterations that might support further classification of the samples between hepatocellular adenoma and hepatocellular carcinoma. Alterations in WNT pathway genes (*CTNNB1*, *APC*, *AXIN1*) were seen in 81% of cases. Non-WNT pathway mutations in *TP53*, *TSC1*, *DNMT3A*, *CREBBP* or various copy-number alterations were present in 56% of atypical hepatocellular neoplasms irrespective of presence or degree of cytoarchitectural atypia. *TERT* promoter mutations and copy-number alterations were restricted to hepatocellular carcinoma (21%). The group proposes that this additional genomic analysis is supported when, by themselves, glutamine synthetase staining and morphology are unable to fully support definitive classification.

### Mutations in cherry hemangiomas

<https://doi.org/10.1038/s41379-019-0284-y>

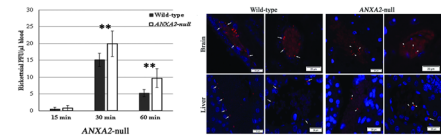


Having observed vascular features of cherry hemangiomas similar to those of anastomosing and congenital hemangiomas, Liao et al. analyzed 68 cherry hemangiomas and 17 hemangioma-like hemangiomas using Sanger sequencing. *GNAQ*, *GNA11* and *GNA14* activating exon 5 mutations were identified in 12, 4, and 32 cherry hemangiomas and 5, 3, and 3 cherry hemangioma-like hemangiomas respectively. Overall, there were equal rates of *GNA* mutation rates between the two groups (82%), and *GNA14* and *GNAQ* mutations were present in 50% of each group. All mutations were mutually exclusive. *GNA14*, *GNAQ*, and *GNA11* were therefore identified as being present in the majority of these very common hemangiomas, establishing a prevalence in these neoplasms, with *GNA14* the most common of the three mutations. The findings confirm that hemangiomas are neoplastic and provide insight into their pathogenesis.

## LABORATORY INVESTIGATION

### ANXA2 in bacterial adhesion

<https://doi.org/10.1038/s41374-019-0284-z>

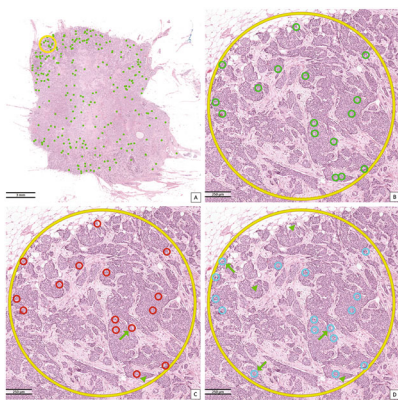


He and colleagues utilized an anatomically based, in vivo, quantitative bacterial adhesion-to-vascular endothelial cells system, combined with atomic force microscopy, to examine the role of endothelial luminal surface ANXA2 during rickettsial adherence to endothelial cells (ECs). They demonstrated mechanisms for bacterial adherence to ECs prior to activation of infection, a previously undescribed mechanism. They also showed that ANXA2 impeded rickettsial attachment to ECs in vitro and blocked rickettsial adherence to blood vessel luminal surface in vivo. EC surface ANXA2 was shown to act as an adherence receptor for rickettsiae, and rickettsial adhesion OmpB was associated with bacterial ligand. The group were able to reduce EC surface-associated *Staphylococcus aureus* by pretreating ECs with anti-ANXA2 antibody, supporting their conclusion that ANXA2 is instrumental in initiating

pathogen–host interactions and bacterial anchoring to vascular luminal surfaces. This provides pathogenic insight and could lead to disrupting this process for both the prevention and treatment of infections.

## Automated mitotic counting

<https://doi.org/10.1038/s41374-019-0275-0>



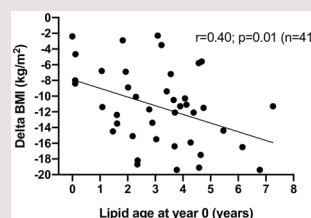
Seeking to minimize subjectivity, Balkenhol et al. assessed deep learning–based automated mitotic counting with fully automated hotspot selection. Two cohorts were compared. Cohort A comprised 90 tumors, selected based on mitotic frequency scores, with pathologists additionally assessing mitotic count in whole-slide images (WSIs) within a selected hotspot. Cohort B comprised 298 tumors for which mitotic frequency was established by three independent observers (averaged) on glass slides. The preselected hotspots in both groups were generated by a convolutional neural network (CNN) trained to detect mitotic figures in digitized hematoxylin and eosin sections. Baseline interobserver agreement for cohort A was kappa 0.689, which increased to 0.814 when CNN-generated hotspots in WSIs were used. Automated counting by the CNN in comparison with observers counting was only slightly lower at 0.724. With optimization, fully automated assessment of mitotic score appears feasible.

## nature.com/pathology

### Adipose lipid turnover and body weight

With studies having established that excess body fat is associated with decreased adipose lipid removal rates, Arner et al. investigated whether lipid turnover was constant over a life span or was influenced by weight gain/loss. Lipid turnover in adults was assessed over a period of up to 16 years by measuring  $^{14}\text{C}$  in adipose tissue triglycerides. Lipid removal decreased with age, with a failure to reciprocally adjust the rate of lipid uptake, often leading to weight gain. Weight loss was driven by rate of lipid uptake rather than the rate of removal, and individuals with low baseline lipid removal rates were more likely to remain weight-stable following weight loss. Adipose turnover is thus a key factor in long-term development of obesity and weight management in humans. Identifying factors affecting lipid turnover is clearly of clinical relevance and instrumental in the maintenance of normal weight as well as maintenance of weight loss.

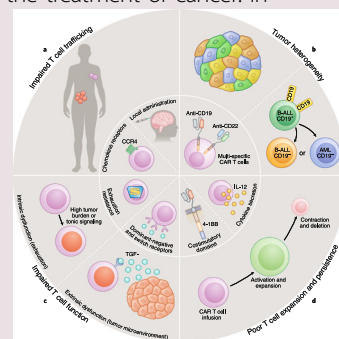
*Nature Medicine* 2019;25:1385–1389; <https://doi.org/10.1038/s41591-019-0565-5>



### Overcoming obstacles in developing CAR T therapeutics

Chimeric antigen receptor (CAR) T-cell therapy for B-cell malignancies is a rapidly expanding and increasingly impressive possibility for the treatment of cancer. In their review, Majzner and Mackall describe a multitude of factors influencing treatment outcome, including histology, regimen, and costimulation. Obstacles include impaired T-cell function (intrinsic and extrinsic), poor T-cell expansion and persistence, tumor heterogeneity, and impaired T-cell trafficking, but the authors note that numerous projects are ongoing to overcome these obstacles. A therapeutic window must be identified for CAR T cells to target antigens shared with normal tissues so as to reduce off-target effects and side effects.

*Nature Medicine* 2019;25:1341–1355; <https://doi.org/10.1038/s41591-019-0564-6>



### Distilling whole-genome histories into composite trees

The task of coming up with systems and algorithms capable of generating useful information from the enormous data sets produced by genome-wide genealogy studies is daunting. This has pushed multiple groups to the forefront and necessitates processing of these enormous data sets down to their individual evolutionary trees. Kelleher et al. introduce an algorithm able to infer whole-genome histories with accuracy comparable to that of current technology while processing four orders of magnitude more sequences, allowing “evolutionary encoding” of the data. Speidel et al. developed a method, Relate, which can scale > 10,000 sequences while simultaneously estimating branch lengths, mutational ages, and variable historical population sizes, allowing inferences of natural selection previously unseen. Both approaches, and others being developed, are instrumental in distilling meaningful genealogical information from genome-wide studies and datasets too large to previously discern such patterns, with wide-ranging implications for evolutionarily structuring studies of the past and future.

*Nature Genetics* 2019;51:1306–1307; <https://doi.org/10.1038/s41588-019-0492-x>

*Nature Genetics* 2019;51:1330–1338; <https://doi.org/10.1038/s41588-019-0483-y>

*Nature Genetics* 2019;51:1321–1329; <https://doi.org/10.1038/s41588-019-0484-x>

